Fermilab FERMILAB-Pub-01/040-A April 2001

A semi-analytical approach to non-linear shock acceleration

Pasquale Blasi [a,1]

[a] *NASA/Fermilab Theoretical Astrophysics Group, Fermi National Accelerator Laboratory, Box 500, Batavia, IL 60510-0500*

Abstract

Shocks in astrophysical fluids can generate suprathermal particles by first order (or diffusive) Fermi acceleration. In the test particle regime there is a simple relation between the spectrum of the accelerated particles and the jump conditions at the shock. This simple picture becomes complicated when the pressure of the accelerated particles becomes comparable with the pressure of the shocked fluid, so that the non-linear backreaction of the particles becomes non negligible and the spectrum is affected in a substantial way. Though only numerical simulations can provide a fully self-consistent approach, a more direct and easily applicable method would be very useful, and would allow to take into account the non-linear effects in particle acceleration in those cases in which they are important and still neglected.

We present here a simple semi-analytical model that deals with these non-linear effects in a quantitative way. This new method, while compatible with the previous simplified results, also provides a satisfactory description of the results of numerical simulations of shock acceleration.

Key words: cosmic rays, high energy, origin, acceleration

1 Introduction

Diffusive shock acceleration is thought to be responsible for acceleration of cosmic rays in several astrophysical environments. Most of the observational evidence for this mechanism, also known as first order Fermi acceleration, has been provided by studies of heliospheric shocks, but there are indirect lines of evidence that acceleration occurs at other shocks. A particularly impressive example was provided a few years ago by the observation of gamma ray

[1] E-mail: blasi@fnal.gov

emission from the supernova remnant SN1006 [1]. These observations could be interpreted as inverse Compton emission of very high energy electrons, accelerated at the shock on the rim of SN1006, though other radiation processes may contribute [2].

Shock acceleration has been studied carefully and a vast literature exists on the topic. Some recent excellent reviews have been written [3–6]. Some of the more problematic aspects of the theory of particle acceleration at astrophysical shocks have been understood, while others are still subject of investigation.

One of the problems that are harder to face is the problem of the injection of particles in the acceleration region. Only particles with a Larmor radius larger than the thickness of the shock are actually able to *feel* the discontinuity at the shock. The shock thickness is of the order of the Larmor radius of thermal protons, so that only a small fraction of the particles can be accelerated.

The calculation of the injection efficiency is quite problematic, for several reasons: first, the distribution function of thermal particles is steeply decreasing with momentum, so that the number of accelerated particles changes wildly with changing injection momentum. Moreover the distribution of the particles in the shock frame is strongly anisotropic at these low momenta, which adds to the difficulty of obtaining a straight analytical answer. Second, the injection of particles from the thermal distribution and their subsequent diffusive transport is thought to be due to the scattering against plasma waves, which are likely to be excited by the particles themselves, which makes the problem intrinsically non-linear. This non-linearity is exacerbated by the backreaction of the particles on the structure of the shocked fluid [7]. The only way to have a complete quantitative picture of the problem of shock acceleration is to use numerical simulations [8,6,9–11].

All these complicated effects, which seem to be important in several astrophysical situations, are nevertheless often neglected, mainly because of the lack of an approach that allows to take them into account without the use of complicated numerical simulations which are usually of restricted use. As a consequence, in most of the applications of the diffusive shock acceleration to astrophysical situations, the assumption of test particles is adopted, even in those cases where this approximation works poorly. Numerical simulations show however that even when the fraction of particles injected from the plasma is relatively small, the energy channelled into these few particles can be close to the kinetic energy of the unshocked fluid, making the test particle approach unsuitable. The most visible effect is on the spectrum of the accelerated particles, which shows a peculiar flattening at the highest energies, due to the backreaction of accelerated particles on the fluid. The consequences on the spectra of secondary particles and radiation processes are clear.

The need to have a theoretical understanding of the non-linear effects in particle acceleration fueled many efforts in finding some *effective* though simplified picture of the problem. The structure of shocked fluids with a backreaction of accelerated particles was investigated in [12–16] in a *fluid* approach. The thermodynamic quantities were calculated including the effects of cosmic rays, but the approach did not provide information on the spectral shape of the accelerated particles.

In Ref. [17] a perturbative approach was adopted, in which the pressure of accelerated particles was treated as a small perturbation. By construction this method provides an answer only for weakly modified shocks.

An alternative approach was proposed in [18–21]. This approach is based on the assumption that the diffusion of the particles is sufficiently energy dependent that different parts of the fluid are affected by particles with different average energies. The way the calculations are carried out implies a sort of separate solution of the transport equation for subrelativistic and relativistic particles, so that the two spectra must be connected at $p \sim mc$ *a posteriori*.

Recently, in [22–24], the effects of the non-linear backreaction of accelerated particles on the maximum achievable energy were investigated, together with the effects of geometry. The solution of the transport equation was written in [24] in an implicit form, and then expanded in terms of the unperturbed (linear) solution.

Recently, some analytical solutions were also presented for the non-linear shock acceleration, in the particular case of Böhm diffusion coefficient [26,27].

The need for a *practical* solution of the acceleration problem in the non-linear regime was recognized in [28], where a simple analytical approximation of the non-linear spectra was presented. In this model the spectrum of the accelerated particles was assumed to consist of a broken power law, with three slopes characterizing the low, intermediate and high energy regimes. The basic features of the spectra derived from numerical simulations were reproduced with this method.

In the present paper we propose an approach that puts together some of the elements introduced in [18], [24] and [28] and provides a semi-analytical solution for the spectrum of accelerated particles and for the structure of the shocked fluid. The method proposed is of simple use, can be adapted to several situations and provides results in very good agreement with numerical simulations, and with simplified models as that in [28].

The paper is structured as follows: in §2 we describe the general problem of linear and non-linear shock acceleration; in §3 we explain in detail our approach to non-linear effects in shock acceleration. In §4 we discuss the results

of our model and compare them with the predictions of the model in Ref. [28] and with the results of some numerical simulations. Our discussion and conclusions are presented in §5.

2 Shock acceleration: linear and non-linear

In this section we discuss the basic elements of shock acceleration and introduce our approach to the description of the non-linear effects due to the backreaction of the accelerated particles on the shocked fluid.

For simplicity we limit ourselves to the case of one-dimensional shocks, but the introduction of different geometrical effects is relatively simple, and in fact many of our conclusions will be not affected by geometry. The non-linear effects are restricted to the mutual action of the shocked fluid and the accelerated particles. In other words, the present work does not include self consistently the production and the absorption of plasma waves by the accelerated particles. This simplification is common to the approaches in [24] and [28].

The equation that describes the diffusive transport of particles in one dimension is

$$\frac{\partial f}{\partial t} = \frac{\partial}{\partial x}\left[D\frac{\partial}{\partial x}f\right] + u\frac{\partial f}{\partial x} + \frac{1}{3}\frac{\partial u}{\partial x}p\frac{\partial f}{\partial p} + Q, \tag{1}$$

where $f(x,p)$ is the distribution function, u is the fluid velocity and D is the diffusion coefficient. The injection of particles is assumed to occur only immediately upstream of the shock, so we write the source function as $Q = Q_0(p)\delta(x)$, where $x = 0$ corresponds to the position of the shock front. For monoenergetic injection, the function $Q_0(p)$ has the following form:

$$Q_0(p) = \frac{N_{inj}u_1}{4\pi p_{inj}^2}\delta(p - p_{inj}), \tag{2}$$

where p_{inj} is the injection momentum and u_1 is the fluid velocity immediately upstream ($u_1 = u(0^+)$). N_{inj} is the number density of particles injected at the shock, parametrized here as $N_{inj} = \eta N_{gas,1}$, where $N_{gas,1}$ is the gas density at $x = 0^+$. The boundary condition at the shock reads:

$$\frac{u_1 - u_2}{3}p\frac{\partial f_0}{\partial p} = \left(D\frac{\partial f}{\partial x}\right)_1 - \left(D\frac{\partial f}{\partial x}\right)_2 + Q_0(p), \tag{3}$$

where u_2 is the fluid velocity downstream. Here we called $f_0 = f(0,p)$ the

distribution function at the shock position.

A useful way of handling eq. (1) was suggested in Ref. [24] (a similar approach was also adopted in Ref. [25]), and consists of integrating this equation in the variable x from $x = 0^+$ (upstream) to $x = +\infty$ (far upstream). After some simple algebraic steps, in which we make use of eq. (3), we obtain the following equation:

$$p\left(\frac{\partial f_0}{\partial p}\right) = -\frac{3}{u_p - u_2}\left\{f_0\left[u_p + \frac{1}{3}\frac{du_p}{d\ln p}\right] - Q_0(p)\right\}, \tag{4}$$

where the stationarity assumption was adopted and we assumed $(D\partial f/\partial x)_2 = 0$. We have introduced the quantity:

$$u_p = u_1 + \frac{1}{f_0(p)}\int_0^\infty dx\left(\frac{du}{dx}\right) f(x,p), \tag{5}$$

and again we called u_1 and u_2 the fluid velocities at $x = 0^+$ and $x = 0^-$ respectively. With this formalism the compression factor at the shock is $R_{sub} = u_1/u_2$. The function u_p, at each momentum p has the meaning of average fluid velocity felt by a particle with momentum p while diffusing upstream. Since the diffusion is in general p-dependent, particles with different energies will *feel* a different compression coefficient, and the correspondent local slope of the spectrum will be p-dependent. Note that, according to eq. (5), the velocity u_p must be a monotonically increasing function of p.

The function u_p describes the mutual interaction between the accelerated particles and the fluid. In other words, if we find the way of determining the function u_p, as we show later, we also determine the spectrum of the accelerated particles.

Eq. (5) is clearly an implicit definition of u_p, meaning that u_p depends on the unknown function f. However, eq. (5) allows us to extract important physical information. For the monoenergetic injection in eq. (2) the solution can be implicitly written as

$$f_0(p) = \frac{N_{inj}q_s}{4\pi p_{inj}^3}\exp\left\{-\int_{p_{inj}}^{p}\frac{dp}{p}\left[\frac{3u_p}{u_p - u_2} + \frac{1}{u_p - u_2}\frac{du_p}{d\ln p}\right]\right\}, \tag{6}$$

where we put (for $\gamma_g = 5/3$):

$$q_s = \frac{3R_{sub}}{R_{sub} - 1}. \tag{7}$$

Eq. (6) tells us that the spectrum of accelerated particles has a local slope given by

$$Q(p) = -\frac{3u_p}{u_p - u_2} - \frac{1}{u_p - u_2}\frac{du_p}{d\ln p}. \tag{8}$$

The problem of determining the spectrum of accelerated particles would then be solved if the relation between u_p and p is found [2]. This is the scope of the next section.

3 The gas dynamics of modified shocks

The velocity, density and thermodynamic properties of the fluid can be determined by the usual conservation equations, including now the pressure of the accelerated particles. We write these equations between a point far upstream ($x = +\infty$), where the fluid velocity is u_0 and the density is $\rho_0 = mN_{gas,0}$, and a generic point where the fluid upstream velocity is u_p (density ρ_p). The index p will denote quantities measured at the point where the fluid velocity is u_p. We call this generic point x_p.

The mass conservation implies:

$$\rho_0 u_0 = \rho_p u_p. \tag{9}$$

Conservation of momentum reads:

$$\rho_0 u_0^2 + P_{g,0} = \rho_p u_p^2 + P_{g,p} + P_{CR,p}, \tag{10}$$

where $P_{g,0}$ and $P_{g,1}$ are the gas pressures at the point $x = +\infty$ and $x = x_p$ respectively, and $P_{CR,p}$ is the pressure in accelerated particles at the point x_p (we used the symbol CR to mean *cosmic rays*, to be interpreted here in a very broad sense). In writing eqs. (9) and (10) we implicitly assumed that the average velocity u_p as defined in eq. (5) coincides with the fluid velocity at the point where the particles with momentum p turn around to recross the shock.

Our basic assumption, similar to that used in [18], is that the diffusion is p-dependent and that therefore particles with larger momenta move farther away from the shock than lower momentum particles. This assumption is expected

[2] In order to determine the spatial distribution of fluid velocity it is necessary to specify the exact diffusion coefficient as function of x and p. In this paper we do need this information, therefore the choice of D does not affect our conclusions.

to describe what actually happens in the case of diffusion dependent on p. As a consequence, at each fixed x_p only particles with momentum larger than p are able to affect the fluid. Strictly speaking the validity of the assumption depends on how strongly the diffusion coefficient depends on the momentum p, but the results should not be critically affected by this assumption. Moreover, in case of strong shocks there are arguments that suggest that the strong turbulence excited by the shock should produce a Böhm diffusion coefficient, so that the dependence $D(p)$ on p should be at least linear.

According to this assumption, only particles with momentum $\gtrsim p$ can reach the point $x = x_p$, therefore

$$P_{CR,p} = \frac{4\pi}{3} \int_p^{p_{max}} dp p^3 v(p) f(p), \tag{11}$$

where $v(p)$ is the velocity of particles whose momentum is p, and p_{max} is the maximum momentum achievable in the specific situation under investigation. In realistic cases, p_{max} is determined from geometry or from the duration of the shocked phase, or from the comparison between the time scales of acceleration and losses. Here we consider it as a parameter to be fixed *a priori*. From eq. (10) we can see that there is a maximum distance, corresponding to the propagation of particles with momentum p_{max} such that at larger distances the fluid is unaffected by the accelerated particles and $u_p = u_0$.

We will show later that for strongly modified shocks the integral in eq. (11) is dominated by the region $p \sim p_{max}$. This improves even more the validity of our approximation $P_{CR,p} = P_{CR}(> p)$. This also suggests that different choices for the diffusion coefficient $D(p)$ may affect the value of p_{max}, but at fixed p_{max} the spectra of the accelerated particles should not be appreciably changed.

Assuming an adiabatic compression of the gas in the upstream region, we can write

$$P_{g,p} = P_{g,0} \left(\frac{\rho_p}{\rho_0} \right)^{\gamma_g} = P_{g,0} \left(\frac{u_0}{u_p} \right)^{\gamma_g}, \tag{12}$$

where we used the conservation of mass, eq. (9). The gas pressure far upstream is $P_{g,0} = \rho_0 u_0^2/(\gamma_g M_0^2)$, where γ_g is the ratio of specific heats ($\gamma_g = 5/3$ for an ideal gas) and M_0 is the fluid Mach number far upstream. Note that eq. (12) cannot be applied at the shock jump, where the adiabaticity condition is clearly violated.

We can rewrite eq. (10) in a convenient way, by dividing it by $\rho_0 u_0^2$ and using

the mass conservation. We then obtain:

$$1+\frac{1}{M_0^2\gamma_g}=U+\frac{1}{M_0^2\gamma_g}U^{-\gamma_g}+\frac{4\pi}{3}\frac{1}{\rho_0 u_0^2}\int_p^{p_{max}} dp' p'^3 v(p') f_0(p') =$$

$$U+\frac{1}{M_0^2\gamma_g}U^{-\gamma_g}+\frac{N_{inj}q_s}{\rho_0 u_0^2 p_{inj}^3}\int_p^{p_{max}} dp' p'^3 v(p') \exp\left\{-\int_{p_{inj}}^{p'}\frac{dp''}{p''}\left[\frac{3u_{p''}}{u_{p''}-u_2}+\frac{1}{u_{p''}-u_2}\frac{du_{p''}}{d\ln p''}\right]\right\}, \quad (13)$$

where we have explicitely written the distribution function $f(p)$ as a power law with local slope $Q(U)$, and we put $U=u_p/u_0$.

Differentiating the previous equation with respect to p we obtain:

$$\frac{dU}{dp}\left[1-\frac{1}{M_0^2}U^{-(\gamma_g+1)}\right]=\frac{1}{3}\frac{N_{inj}q_s}{\rho_0 u_0^2}\left(\frac{p}{p_{inj}}\right)^3 v(p)\exp\left\{-\int_{p_{inj}}^{p}\frac{dp}{p}\left[\frac{3u_p}{u_p-u_2}+\frac{1}{u_p-u_2}\frac{du_p}{d\ln p}\right]\right\} \quad (14)$$

or

$$\frac{dU}{d\ln p}\left[1-\frac{1}{M_0^2}U^{-(\gamma_g+1)}\right]=$$

$$\frac{1}{3}\frac{N_{inj}q_s}{\rho_0 u_0^2}v(p)p_{inj}\exp\left\{4\ln\left(\frac{p}{p_{inj}}\right)-\int_{p_{inj}}^{p}\frac{dp}{p}\left[\frac{3u_p}{u_p-u_2}+\frac{1}{u_p-u_2}\frac{du_p}{d\ln p}\right]\right\}. \quad (15)$$

Note that the velocity u_p changes as a consequence of the pressure added by non-thermal particles, therefore the function $U(p)$ must be a monotonically increasing function of the particle momentum. Since $U(p)$ and $dU/d\ln p$ are always non-zero, we can calculate their logarithm, so that eq. (15) becomes:

$$\ln \mathcal{D}U+\ln\left[1-\frac{1}{M_0^2}U^{-(\gamma_g+1)}\right]$$

$$=\ln\left[\frac{1}{3}\frac{N_{inj}q_s}{\rho_0 u_0^2}v(p)p_{inj}\right]+4\ln\left(\frac{p}{p_{inj}}\right)-\int_{p_{inj}}^{p}\frac{dp}{p}\left[\frac{3R_{tot}U}{R_{tot}U-1}+\frac{R_{tot}}{R_{tot}U-1}\mathcal{D}U\right], \quad (16)$$

where we put $\mathcal{D}U=dU/d\ln p$. The following equality is easily demonstrated:

$$\int_{p_{inj}}^{p}\frac{dp}{p}\frac{R_{tot}}{R_{tot}U-1}\mathcal{D}U=\ln\left(\frac{R_{tot}U-1}{R_{sub}-1}\right), \quad (17)$$

so that the equation for $\mathcal{D}U$ becomes:

$$\ln \mathcal{D}U + \ln\left[1 - \frac{1}{M_0^2} U^{-(\gamma_g+1)}\right]$$

$$= \ln\left[\frac{1}{3}\frac{N_{inj} q_s}{\rho_0 u_0^2} v(p) p_{inj}\right] + 4\ln\left(\frac{p}{p_{inj}}\right) - \ln\left(\frac{R_{tot}U - 1}{R_{sub} - 1}\right) - \int_{p_{inj}}^{p} \frac{dp}{p}\frac{3R_{tot}U}{R_{tot}U - 1} \quad (18)$$

Solving this differential equation provides $U(p)$ and therefore the spectrum of accelerated particles, through eq. (6).

The operative procedure for the calculation of the spectrum of accelerated particles is simple: we fix the boundary condition at $p = p_{inj}$ such that $U(p_{inj}) = u_1/u_0$ for some value of u_1 (fluid velocity at $x = 0^+$). The evolution of U as a function of p is determined by eq. (18). The physical solution must have $U(p_{max}) = 1$ because at $p \gtrsim p_{max}$ there are no accelerated particles to contribute any pressure. There is a unique value of u_1 for which the fluid velocity at the prescribed maximum momentum p_{max} is $u_{p_{max}} = u_0$ (or equivalently $U(p_{max}) = 1$). Finding this value of u_1 completely solves the problem, since eq. (18) provides $U(p)$ and therefore the spectrum of accelerated particles, calculated according to eq. (4). Conservation of energy can be easily checked.

An illustration of this procedure is presented in fig. 1 where we considered the following special set of parameters: the Mach number far upstream is $M_0 = 43$, and the gas temperature is $T_0 = 10^6$ K, corresponding to $u_0 = 5 \times 10^8$ cm/s. The parameter η is taken to be 4×10^{-3}, and the injection of particles occurs at $p_{inj} = 10^{-2}mc$, where m is the mass of the accelerated particles. In this paper we assume that the accelerated particles are protons. The maximum momentum is $p_{max} = 10^5 mc$. The three curves which are plotted correspond to the function $U(p)$ for $R_{sub} = 2$ (dotted line), $R_{sub} = 1.5$ (dashed line) and $R_{sub} = 1.817$ (solid line). It is immediately evident that only for $R_{sub} = 1.817$ the function $U(p)$ reaches unity at $p = p_{max}$. Our method then provides the value of R_{sub} and consequently the values of the other parameters.

Fig. 1 is very useful for understanding the physical meaning of the local velocity u_p. Particles with large momenta *feel* compression factors u_p/u_2 which are larger than those felt by low momentum particles. Large compression factors correspond to locally flatter spectra, so that the spectrum of accelerated particles is expected to become flatter at large momenta. We define the total compression factor $R_{tot} = u_0/u_2$. Note that the compression factor at the gas subshock is now $R_{sub} \ll 4$, the value expected for a strong shock in the test particle regime.

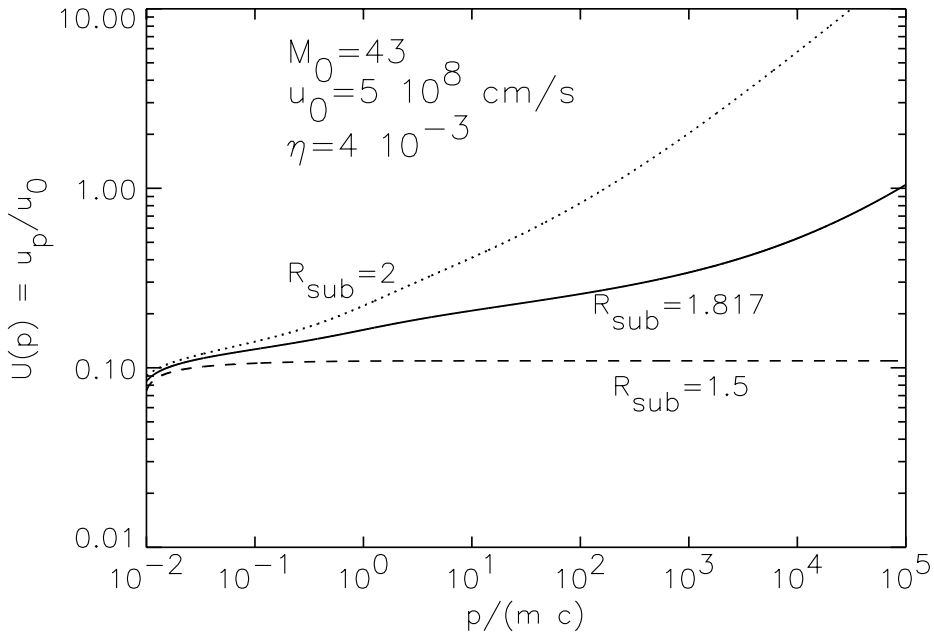

Fig. 1. *$U(p)$ as a function of momentum, for different values of the compression factor at the subshock. The fluid dynamics must be unaffected at $p = p_{max}$ which implies that $U(p_{max}) = 1$. This condition determines the right value of R_{sub}.*

4 Results

The calculations illustrated in the previous section are here tested versus previous models and numerical simulations. In particular we compare our results with the predictions of the simple approach presented in [28], that we briefly summarize. In [28] the spectrum of accelerated particles has a prescribed shape, made of three power laws, in the low ($p_{inj} \leq p \leq mc$), intermediate ($mc \leq p \leq 10^{-2} p_{max}$) and high ($10^{-2} p_{max} \leq p \leq p_{max}$) energy regimes. The slope in the three regions is then calculated by requiring mass, momentum and energy conservation.

We first check that our model reproduces the results in the linear regime, where the test particle approximation can be adopted, and then we study the transition to the non-linear regime. For this purpose, we consider a shock with Mach number $M_0 = 5$, with a gas temperature $T_0 = 10^8$ K. We choose $p_{inj} = 10^{-2} mc$ and $p_{max} = 10^5 mc$, and we study the result for different values of η, as plotted in Fig. 2. The solid line is obtained for $\eta = 10^{-5}$; our model gives for this case $R_{sub} = R_{tot} = 3.57$, which is exactly the value obtained from test particle theory: $R_{sub} = (8M_0/3)/((2/3)M_0 + 2)$, for $\gamma_g = 5/3$. The test particle approximation would provide the same compression factor for any value of η. Our results for $\eta = 10^{-3}$ and $\eta = 10^{-2}$ are plotted in Fig. 2 as dotted and dashed lines respectively. These two cases result in $(R_{sub}, R_{tot}) = (3.45, 3.83)$

for $\eta = 10^{-3}$ and $(R_{sub}, R_{tot}) = (2.85, 4.49)$ for $\eta = 10^{-2}$. The transition from unmodified shocks to strongly modified shocks is evident.

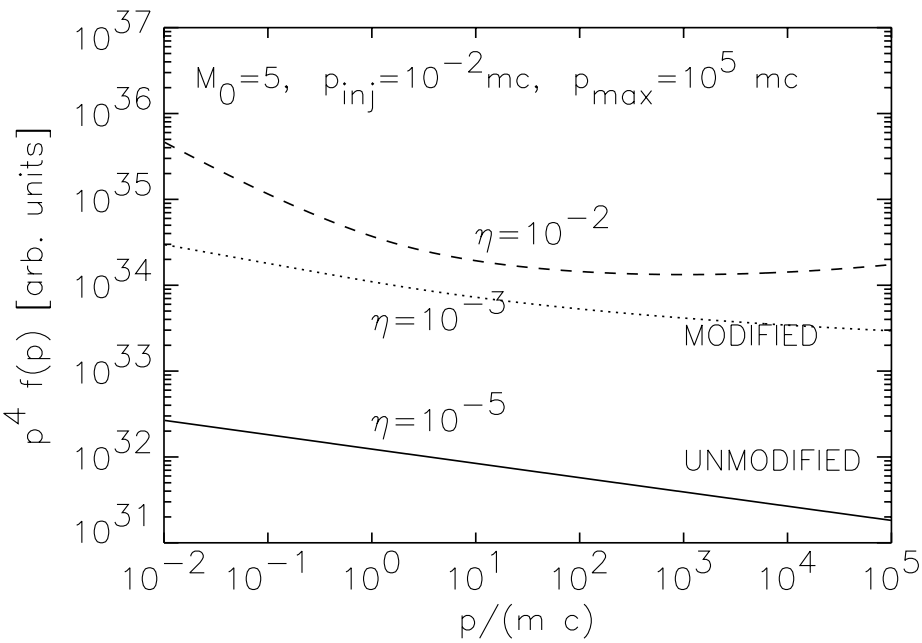

Fig. 2. *Spectra of accelerated particles for low Mach number ($M_0 = 5$). Increasing the value of η determines the transition from an unmodified shock (solid line, $\eta = 10^{-5}$) and a modified shock (dashed and dotted lines, with $\eta = 10^{-2}$ and $\eta = 10^{-3}$ respectively).*

In all the cases the common feature of the modified shocks is a steepening of the spectrum (in comparison with the linear result) at low energy and a flattening at high energies. From the phenomenological point of view this can be of paramount importance since it may change the spectral features of the secondary radiation produced by the interactions of the accelerated particles.

The more interesting case is that of strongly modified shocks, where we expect the pressure in accelerated particles to become comparable with the kinetic energy of the upstream fluid. Intuitively this is mainly the case for high Mach number shocks, though we also show that there are exceptions. We can compare our results with those of the model in Ref. [28].

Let us consider the case $M_0 = 43$, $u_0 = 5 \times 10^8$ cm/s, $p_{inj} = 10^{-2}mc$, and let us study the resulting spectra for $\eta = 10^{-3}$ and different values of p_{max}. The results are plotted in Fig. 3.

The results of [28] are plotted in the form of crosses ($p_{max} = 10^3 mc$), stars ($p_{max} = 10^5 mc$) and diamonds ($p_{max} = 10^7 mc$). The corresponding continuous lines are the results of our model.

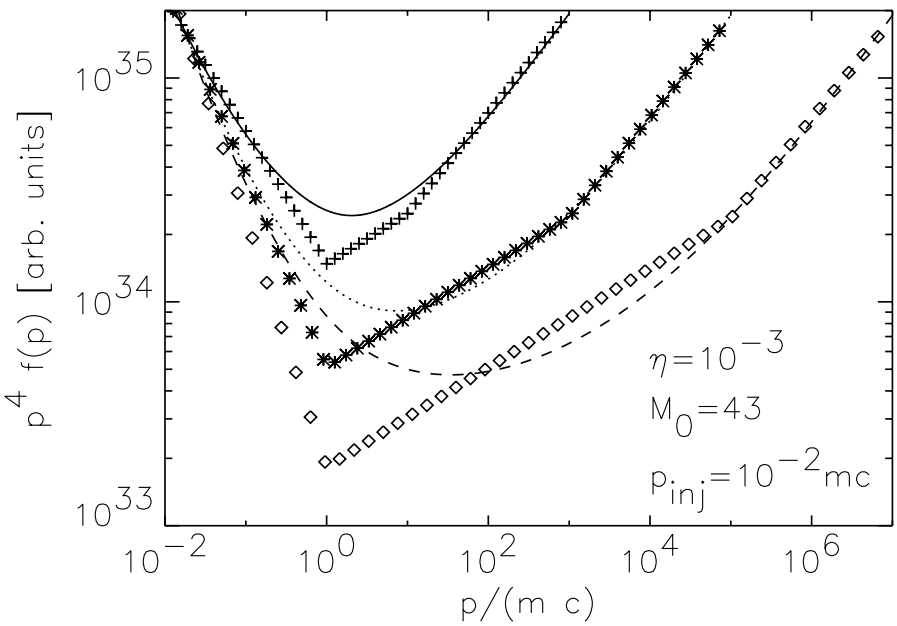

Fig. 3. *Comparison between the prediction of our model (lines) and those of Ref. [28] (symbols). The three sets of curves are obtained for* $p_{max} = 10^3 mc$ *(solid line and crosses),* $p_{max} = 10^5 mc$ *(dotted line and stars) and* $p_{max} = 10^7 mc$ *(dashed line and diamonds).*

Some comments are in order: the slope of the spectrum of accelerated particles predicted in our model at $p \sim p_{max}$ is approximately equal to that obtained in [28]. This is not surprising since the model in [28] is based on a three power law approximation, and the slope of the spectrum at the highest energies is calculated using an asymptotic expression derived from eq. (6). At low values of p_{max} our results are in very good agreement with the general features of the solutions in [28]. At increasingly larger values of p_{max} the agreement is not extremely good but still reasonable, if one takes into account that the following three assumptions were made in [28]: 1) the velocity of the particles is assumed to be p/m for $p \leq mc$ and equal to c for $p \geq mc$; 2) the momentum at which there is a change in slope at low energy is forced to be at $p = mc$; 3) the position of the point where there is the change in slope at intermediate energies is forced to be at $p = 10^{-2} p_{max}$. In our model all the three assumptions are released and the spectra are smooth. This is the reason for the slightly different position of the dip in our spectra ($p^4 f(p)$) when compared with those derived according to [28]. Similar conclusions hold for different values of the parameters.

A more interesting comparison, to test the effectiveness of our model is that with the results of numerical simulations. Since a similar comparison was carried out in [28] to test that model, we consider here the same situation,

so that a full cross-check is possible. The case we consider is that of a shock with Mach number $M_0 = 128$ and a fluid temperature of $T = 10^6$ K. The results provided by a numerical simulation are plotted in Fig. 5 of Ref. [28] and reproduced in our Fig. 4 as a dashed line. From the simulation we can extract the values of some parameters: the injection momentum is $p_{inj} = 7 \times 10^{-3} mc$, while the maximum momentum is $p_{max} = 10^5 mc$. Note that the simulation does not provide these parameters in a clear way, because there the thermal and non-thermal particles are treated in the same way, therefore some approximation is involved in deriving these numerical values. The best fit of the model in [28] to the results of the simulation implies $R_{sub} = 2.68$ and $R_{tot} = 52$ using $\eta = 5 \times 10^{-3}$. Using the same value of the injection efficiency η, our model predicts $R_{sub} = 2.365$ and $R_{tot} = 51.9$. The spectra for the model in [28] and for our model are plotted in Fig. 4 as a solid light broken line, and as a thick solid line respectively. The improvement provided by our model is evident (note that we only used the values of η and p_{inj} derived in [28], though an even better agreement can be found by slightly changing these values, that, as we stressed above, are not clearly determined by the simulation).

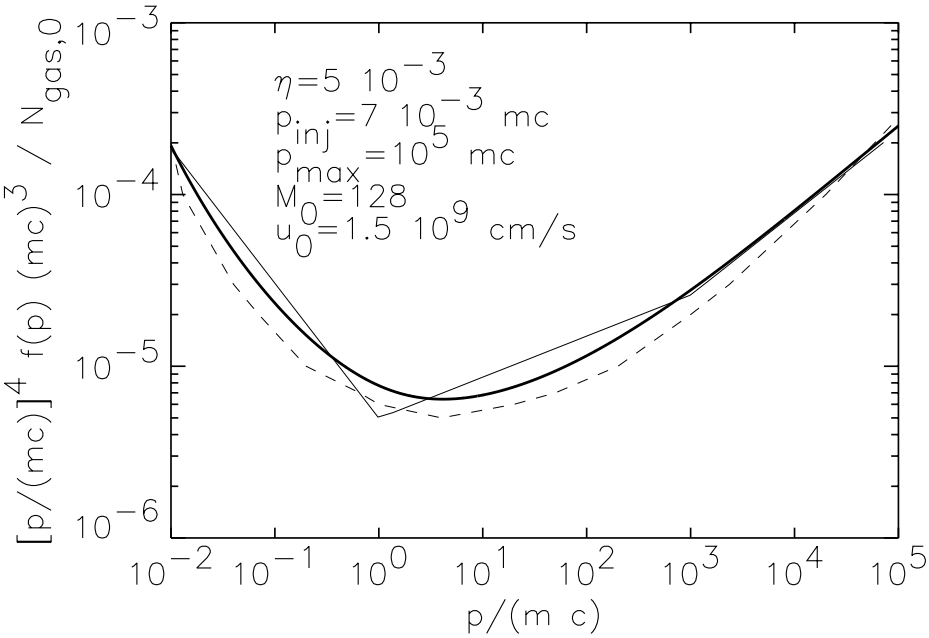

Fig. 4. *Comparison between the predictions of our model (thick solid line) and the results of simulations (dashed line) and the approximation in Ref. [28] (solid light line).*

A basic issue raised in [28] is that of the accurate description of the slope of the spectrum of accelerated particles at $p \sim p_{max}$. The importance of this point is due to the flat spectral shape at high momenta, which gives the main contribution to the total energy budget in accelerated particles, for strongly modified shocks. We show our prediction for the local slope in Fig. 5, as a

function of the momentum. The most noticeable feature of this figure is the slope ~ 3.5 at $p \sim p_{max}$, very close to that predicted by numerical simulations.

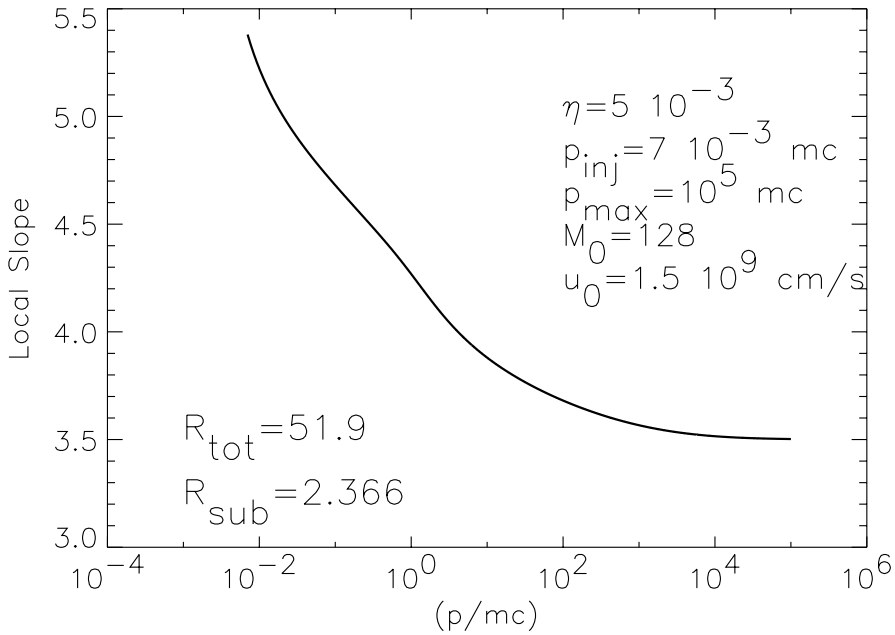

Fig. 5. *Slope of the spectrum of accelerated particles according with our model, with the parameters used to obtain the curves in Fig. 4.*

One comment is in order concerning the injection: in all the cases considered above, the injection momentum and η, the injection efficiency, are chosen independently. In a realistic case (for instance in the simulation) the two parameters would be actually related to each other. For instance, if the particles are extracted from the thermal distribution, then one can write in a very general way, that the injection momentum is proportional to the sound speed downstream ($c_{s,2}$), times the particle mass, $p_{inj} = \xi m c_{s,2}$. The parameter ξ must be large enough that the particles can *feel* the thickness of the shock, determined either by the interaction pathlength of the particles, or by the Larmor radius of the thermal protons in the local magnetic field. Hence, ξ must be at least a few, and indeed it is usually assumed to be in the range $\xi \sim 4 - 10$. If the expression $p_{inj} = \xi m c_{s,2}$ is adopted, and the injection is assumed to occur from the thermal distribution, then the parameter η is no longer free, and can be determined self-consistently. However it is wise to keep in mind that in this case η would change wildly for small changes in ξ, due to the exponential suppression in the distribution function at momenta larger than the thermal average.

We continue now the analysis of the predictions of our model and the comparison with the results of Ref. [28]. An important issue is that of determining where the transition from unmodified to strongly modified shock occurs, as a

function of the parameters of the calculation.

In Fig. 6 we plot the compression ratios (total and at the subshock) for different values of the maximum momentum of the accelerated particles. The solid lines represent the results of our model, compared with the values predicted by the simple approach in [28] (dashed lines). There is a good agreement between the two approaches. For $\eta = 10^{-3}$ the shock becomes strongly modified already for p_{max} a few times larger than mc, confirming that even relatively low injection efficiencies cause the shock to be affected by the backreaction of the accelerated particles.

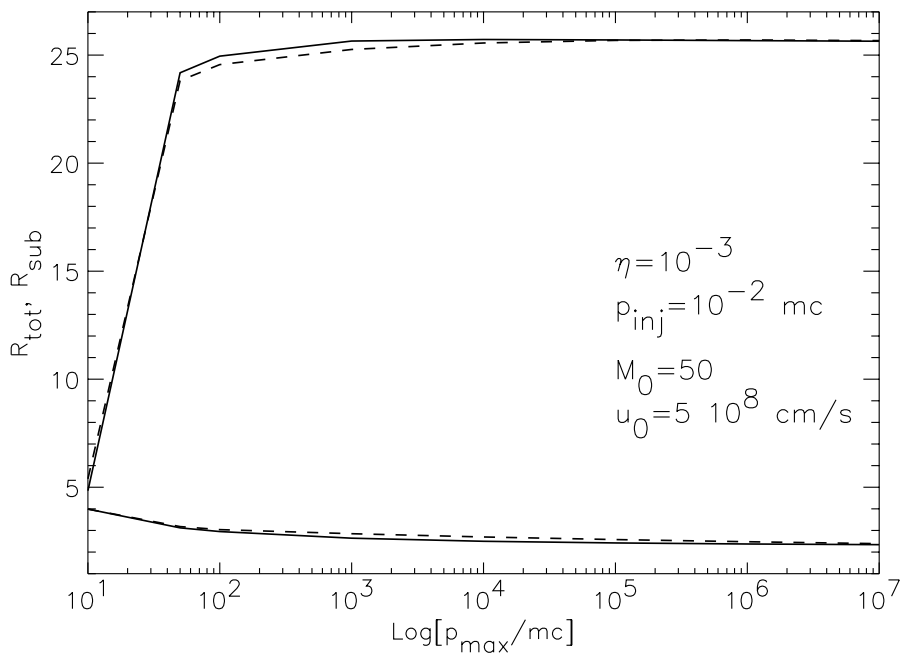

Fig. 6. *Compression factors according with our model (solid lines) and the simple model (dashed lines), as functions of p_{max}, for the values of the parameters reported in the figure. The upper curves represent R_{tot} and the lower curves represent R_{sub}.*

In Fig. 7 the same compression factors are plotted versus the minimum (injection) momentum p_{inj}. Here some differences between our model and that in Ref. [28] are visible. The results can be interpreted as an evidence that our model predicts the onset of the modified shock phase, at slightly larger values of p_{inj} compared to the simple model.

The results of a similar study are plotted in Fig. 8, where the dependence of R_{tot} and R_{sub} is investigated versus the injection efficiency η. Again, our model predicts that the shock starts to be modified at values of η slightly larger than for the simplified model. In particular for the values of the parameters reported in Fig. 8, we obtain that the shock starts to be modified at $\eta \gtrsim 10^{-4}$, while the simple model gives a modified shock for $\eta \gtrsim 3 \times 10^{-5}$. Finally in

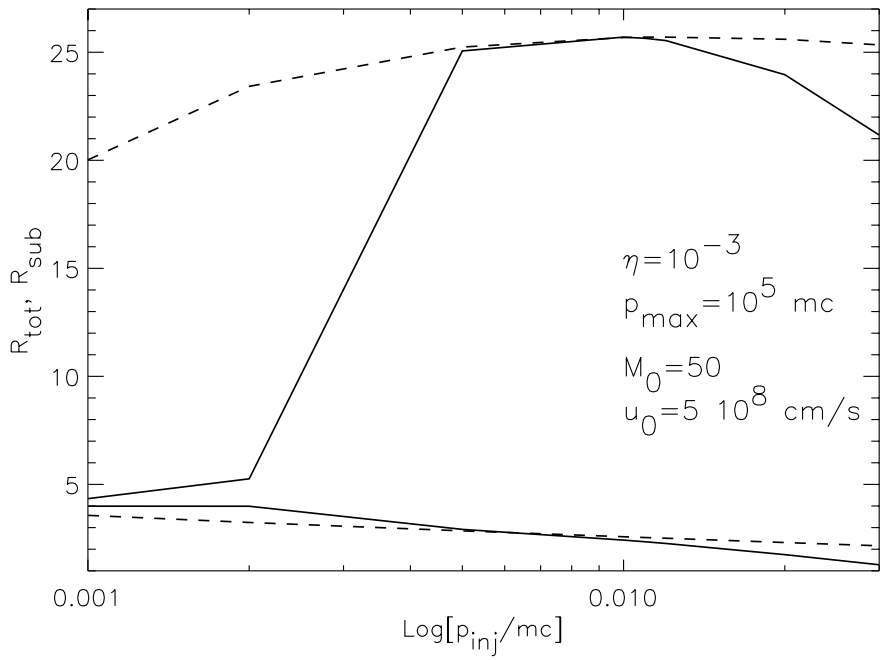

Fig. 7. *Compression factors according with our model (solid lines) and the simple model (dashed lines) as functions of the injection momentum. The upper curves represent R_{tot} and the lower curves represent R_{sub}.*

Fig. 9 we investigate the dependence of R_{tot} and R_{sub} on the Mach number of the fluid at infinity (upstream). We specialize our prediction to the case $\eta = 10^{-3}$, $p_{inj} = 10^{-2}mc$ and $p_{max} = 10^5 mc$, but clearly similar plots can be produced for different regions of the parameter space. The results of our model are in very good agreement with the results of [28]. Our model however predicts a slightly lower value of the critical Mach number M_{cr}, above which the shock is no longer modified, so that R_{tot} and R_{sub} settle down at the usual (linear) value of ~ 4. As found in [28], the relation between R_{tot} and M_0 is $R_{tot} \propto M_0^{3/4}$, for $M_0 \leq M_{cr}$.

5 Discussion and Conclusions

We proposed a semi-analytical method to calculate the spectrum of particles accelerated at shocks, and the velocity profile of the shocked fluid, including the non-linear effects due to the backreaction of the non-thermal particles on the dynamics of the shocked fluid.

The approach presented in this paper provides results that are in good agreement with the output of numerical simulations on shock acceleration and also with the results of a previous model aimed to a simple description of the non-

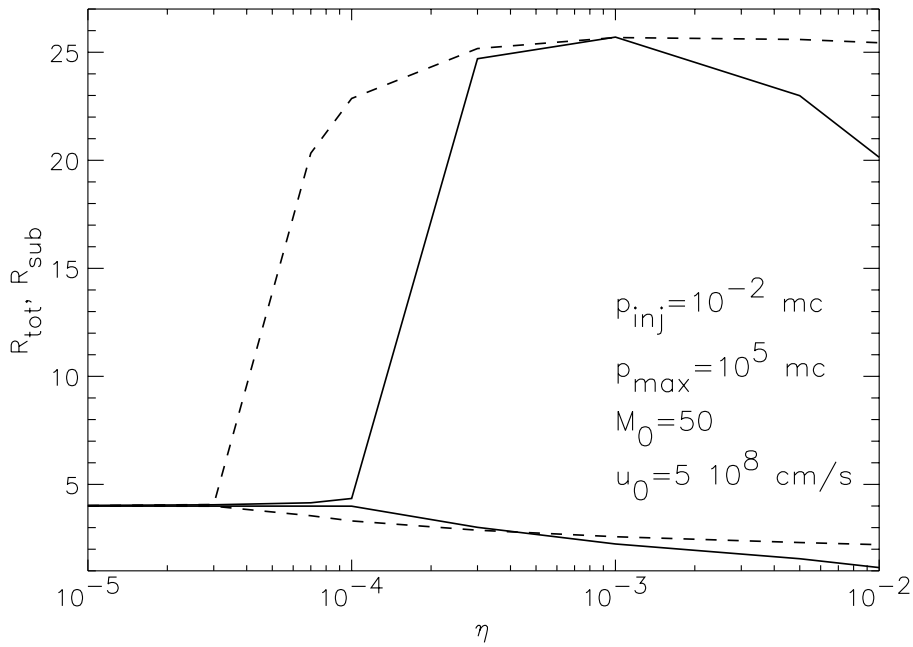

Fig. 8. *Compression factors according with our model (solid lines) and the simple model (dashed lines) as functions of the injection efficiency η. The upper curves represent R_{tot} and the lower curves represent R_{sub}.*

linear effects [28]. Compared with the latter, our model provides a better fit to numerical results, and is not based on *a priori* assumptions on the spectrum of accelerated particles in some energy ranges.

We confirm the main results on shock acceleration, known from simple models and from simulations: *i)* the backreaction of the accelerated particles is important, even in those cases in which a small fraction of the particles injected at the shock is actually accelerated to suprathermal energies. For $\eta \gtrsim 10^{-4}$ the shock becomes modified by the non-thermal pressure and both the velocity field of the shocked fluid and the spectrum of the accelerated particles are affected. The minimum value of η for which the shock is modified in our model is slightly larger than that predicted in [28]. *ii)* For linear shocks the maximum compression factor that can be achieved is 4 (for $\gamma_g = 5/3$) which corresponds to spectra $\propto p^{-4}$. This result is obtained for $M_0 \to \infty$. When the backreaction becomes relevant, the structure of the shocked fluid is changed into a smooth decrease of the fluid speed from u_0 at infinity (effectively at some distance D_{max}) to u_1 at the position of the gas (ordinary) subshock. While at the subshock it is still true that the maximum compression factor is 4, the overall compression factor (R_{tot}) between downstream and D_{max} can be arbitrarily large. *iii)* The large total compression factors for strongly modified shocks result in a flattening of the spectra of accelerated particles at high energy. The slope there tends to ~ 3.5 (flatter than 4). The slope of the spectrum at low

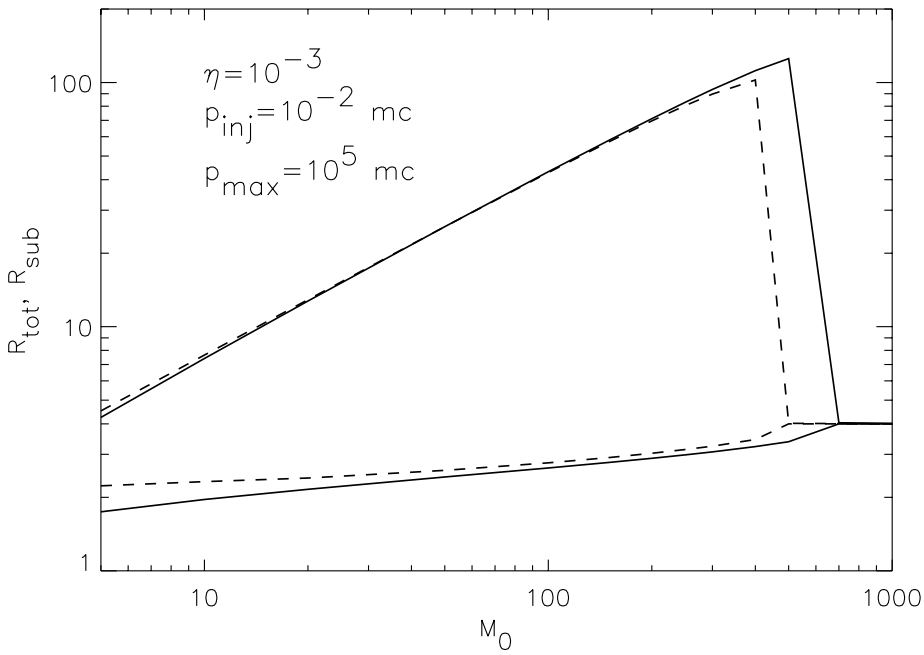

Fig. 9. *Compression factors according with our model (solid lines) and the simple model (dashed lines) as functions of the Mach number M_0. The upper curves represent R_{tot} and the lower curves represent R_{sub}.*

energy is determined by the compression factor at the subshock, and is usually steeper than the slope predicted in linear theory. *iv)* In general, increasing the Mach number corresponds to an increasingly more modified shock, up to a critical Mach number M_{cr}. At $M > M_{cr}$, the total and subshock compression factors both converge to the linear value of 4 and the shock behaves as an ordinary strong shock (it is no longer an efficient accelerator).

Although the calculations reported in the paper refer to the case of a plane (one dimensional) shock and the effects of waves (Alfvèn heating) have not been included, these changes are almost straightforward. In fact, for spherical shocks, the expression for the distribution function $f_0(p)$ remains unchanged [eq. (6)], although the definition of u_p is formally different (it reflects the geometry). All the rest of the calculation remains unaffected and most of the results still hold. The case of spherical symmetry would be relevant for shocks related to supernova remnants, as discussed in [24].

The introduction of the heating due to damping of Alfvén waves implies a change in the relation between $P_{g,p}$ and $P_{g,0}$ but this change can be easily written in a way which is useful for our purposes. For instance, generalizing a discussion in [28], in the approximation of large Alfvén Mach number ($M_A = u_0/v_A$, where v_A is the Alfvén speed, assumed constant in all the fluid) we can

write

$$\frac{P_{g,p}}{P_{g,0}} \simeq \left(\frac{\rho_p}{\rho_0}\right)^{\gamma_g} \left\{1 + (\gamma_g - 1)\frac{M_0^2}{M_A}\left[1 - \left(\frac{\rho_0}{\rho_p}\right)^{\gamma_g}\right]\right\}. \tag{19}$$

Clearly the effects of Alfvén heating can be neglected as long as $M_0^2 \ll M_A$. Introducing eq. (19) [instead of eq. (12)] in eq. (10), it is easy to derive an equation similar to eq. (18), that can be solved for $U(p)$. The spectrum of accelerated particles is then obtained using the same procedure illustrated above. The basic effect of the Alfvén heating is to reduce the total compression factors, and make the spectra at high energy slightly steeper than found in §4.

We conclude by stressing that the non-linear effects discussed here appear to be relevant even for a small injection efficiency, and their phenomenological consequences can be critically important. For instance, as an application of the simple model presented in [28], in Ref. [29] the spectra of secondary radio and gamma radiation in supernova remnants were calculated. The differences with respect to the results obtained by adopting the test particle approximation are impressive.

In this prospective, the semi-analytical model presented here, being of easy use and having an immediate physical interpretation, provides the suitable tool to estimate the phenomenological consequences of non-linearity in shock acceleration, in the cases where it is unpractical to have access to numerical simulations.

Acknowledgments This work was supported by the DOE and the NASA grant NAG 5-7092 at Fermilab.

References

[1] T. Tanimori, et al., Astrophys. J. Lett. 497 (1998) L25.

[2] F.A. Aharonian, and A.M. Atoyan, Astron. & Astroph. 351 (1999) 330.

[3] L.O'C. Drury, Rep. Prog. Phys. 46 (1983) 973.

[4] R.D. Blandford, and D. Eichler, Phys. Rep. 154 (1987) 1.

[5] E.G. Berezhko, and G.F. Krimsky, Soviet. Phys.-Uspekhi, 12 (1988) 155.

[6] F.C. Jones, and D.C. Ellison, Space Sci. Rev. 58 (1991) 259.

[7] A.R. Bell, MNRAS 225 (1987) 615.

[8] D.C. Ellison, E. Möbius, and G. Paschmann, Astrophys. J. 352 (1990) 376.

[9] D.C. Ellison, M.G. Baring, and F.C. Jones, Astrophys. J. 453 (1995) 873.

[10] D.C. Ellison, M.G. Baring, and F.C. Jones, Astrophys. J. 473 (1996) 1029.

[11] H. Kang, and T.W. Jones, Astrophys. J. 476 (1997) 875.

[12] L.O'C Drury, and H.J. Völk, Proc. IAU Symp. 94 (1980) 363.

[13] L.O'C Drury, and H.J. Völk, Astrophys. J. 248 (1981) 344.

[14] L.O'C Drury, W.I. Axford, and D. Summers, MNRAS 198 (1982) 833.

[15] W.I. Axford, E. Leer, and J.F. McKenzie, Astron. & Astrophys. 111 (1982) 317.

[16] P. Duffy, L.O'C Drury, and H. Völk, Astron. & Astrophys. 291 (1994) 613.

[17] R. Blandford, Astrophys. J. 238 (1980) 410.

[18] D. Eichler, Astrophys. J. 277 (1984) 429.

[19] D. Ellison, and D. Eichler, Astrophys. J. 286 (1984) 691.

[20] D. Eichler, Astrophys. J. 294 (1985) 40.

[21] D.C. Ellison, and D. Eichler, Phys. Rev. Lett. 55 (1985) 2735.

[22] E.G. Berezhko, V.K. Yelshin, and L.T. Ksenofontov, Astropart. Phys. 2 (1994) 215.

[23] E.G. Berezhko, L.T. Ksenofontov, and V.K. Yelshin, Nucl. Phys. B (Proc. Suppl.) 39A (1995) 171.

[24] E.G. Berezhko, Astropart. Phys. 5 (1996) 367.

[25] G. Pelletier, and J. Roland, Astron. & Astroph. 163 (1986) 9.

[26] M.A. Malkov, Astrophys. J. 485 (1997) 638.

[27] M.A. Malkov, P.H. Diamond and H.J. Völk, Astrophys. J. 533 (2000) 171.

[28] E.G. Berezhko, and D.C. Ellison, Astrophys. J. 526 (1999) 385.

[29] D.C. Ellison, E.G. Berezhko, and M.G. Baring, Astrophys. J. 540 (2000) 292.